Laser-based surface preparation of composite laminates leads to improved electrodes for electrical measurements

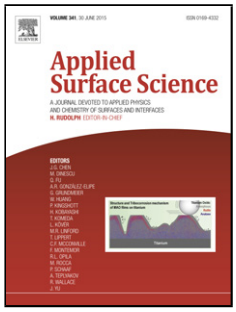

Title: Laser-based surface preparation of composite laminates leads to improved electrodes for electrical measurements

Author: Khaled Almuhammadi Lakshmi Selvakumaran Marco Alfano Yang Yang Tushar Kanti Bera Gilles Lubineau

PII: S0169-4332(15)02505-2
DOI: http://dx.doi.org/doi:10.1016/j.apsusc.2015.10.086
Reference: APSUSC 31567

To appear in: *APSUSC*

Received date: 23-7-2015
Revised date: 11-10-2015
Accepted date: 14-10-2015

Please cite this article as: Khaled Almuhammadi, Lakshmi Selvakumaran, Marco Alfano, Yang Yang, Tushar Kanti Bera, Gilles Lubineau, Laser-based surface preparation of composite laminates leads to improved electrodes for electrical measurements, *Applied Surface Science* (2015), http://dx.doi.org/10.1016/j.apsusc.2015.10.086

Laser-based surface preparation of composite laminates leads to improved electrodes for electrical measurements

Khaled Almuhammadi[a], Lakshmi Selvakumaran[a], Marco Alfano[b], Yang Yang[c], Tushar Kanti Bera[a], Gilles Lubineau[a,*]

[a] *King Abdullah University of Science and Technology (KAUST), Physical Sciences and Engineering Division, COHMAS Laboratory Thuwal 23955-6900. Saudi Arabia*

[b] *Department of Mechanical, Energy and Management Engineering, University of Calabria, Via P. Bucci 44C, 87036 Rende (CS), Italy*

[c] *King Abdullah University of Science and Technology (KAUST), Imaging and Characterization Core Laboratory Thuwal 23955-6900. Saudi Arabia*

Abstract

Electrical impedance tomography (EIT) is a low-cost, fast and effective structural health monitoring technique that can be used on carbon fiber reinforced polymers (CFRP). Electrodes are a key component of any EIT system and as such they should feature low resistivity as well as high robustness and reproducibility. Surface preparation is required prior to bonding of electrodes. Currently this task is mostly carried out by traditional sanding. However this is a time consuming procedure which can also induce damage to surface fibers and lead to spurious electrode properties. Here we propose an alternative processing technique based on the use of pulsed laser irradiation. The processing parameters that result in selective removal of the electrically insulating resin with minimum surface fiber damage are identified. A quantitative analysis of the electrical contact resistance is presented and the results are compared with those obtained using sanding.

Keywords: A. Laminates, B. Electrical properties, C. Surface electrodes, D. Laser ablation

*Email address: gilles.lubineau@kaust.edu.sa

1. Introduction

In recent times the use of modern composite materials is becoming increasingly widespread. However, the failure modes of composite structures are extremely complex and, unlike metals, they may suffer significant degradation with barely visible surface damage. Since the damage may cause serious decrease in material strength and lead to catastrophic failure, the development of reliable structural health monitoring (SHM) techniques is crucial and has a tremendous impact on the life-cycle cost spent for inspection and repair [8].

As a result, a number of nondestructive evaluation techniques have been put forward, including dielectric spectroscopy [48], ultrasonic evaluation [13, 45, 18], vibration analysis [13], phased array analysis [13], shearography [13], thermography [13, 14], infrared thermography [11], ultrasonic phased array [55], sampling phased array (SPA) [55], synthetic aperture focusing technique (SAFT) [55], flash thermography [10], dynamic modulus measurements [35], and acoustic emission monitoring [2, 25].

Techniques based on changes in electrical properties (*i.e.* electrical resistance or impedance methods) [34, 5, 6] have been found to be fast and low-cost methods that are suitable for offline or online inspection of carbon fiber reinforced polymer (CFRP) composites. Electrical impedance tomography (EIT) can be non-invasive and used for *in-situ* and real-time monitoring of structural integrity in terms of electrical impedance. Unlike other classical methods, such as optical fiber grating [24], ultrasonic [18], acoustic emission [25], and modal analysis [9], EIT does not require highly sensitive external sensors and/or actuators or costly equipment.

One of the main components of an EIT system is the electrode array which acts as an interface between the external hardware and the structure. To monitor structural health, a constant current is supplied through a set of electrodes and then electric potentials are collected from subsequent pairs of electrodes. Variations in electric potential profiles obtained from the two measurement cycles are used to reconstruct the corresponding variation of conductivity in the domain of interest [47, 1]. The obtained conductivity image can then be used to assess the type and extent of local damage in the tested volume provided

the relationships between the damage level and the (generally anisotropic) local change in conductivity are known. This task can be accomplished through the solution of an inverse problem and the required relationships have recently been reported in [37, 21, 38]. It follows that the outcome of the reconstruction process depends on the robustness of the system and the accuracy of the data which, in turn, rely on the quality of the interface between the electrical hardware and the structure being monitored *i.e.* the electrodes.

A high-quality electrode should possess the following characteristics: (i) the interfacial bonding should be strong and uniform; (ii) the contact impedance should be low; (iii) the electrode material should be highly conductive; (iv) the durability of the electrode should be long term, *i.e.* the electrode should not debond with time/load so that the electrical resistance of the interface can be considered low, uniform and stable over the time; (v) the fabrication steps should be easy to reproduce; and (vi) the coupling of the electrode to the laminate should not induce any damage or create a hot spot in the structure. Additional factors that have important implications, in terms of both processing and practice, are the electrode's low cost and easy mass production with minimal manual intervention. Here, electrodes used for EIT of composite laminates are obtained in four main steps: (1) surface preparation, (2) bonding of the electrode to the structure, (3) electrical wiring and (4) coating with an insulating and protective material. Surface preparation and bonding are the most important steps. Surface preparation involves removal of the surface resin to expose the conductive carbon fibers to which the highly conductive electrode material will be bonded. This step is very important because the main conducting elements in a CFRP composite are often the carbon fibers which must be connected to the electrodes. Materials commonly used in the electrodes are silver paste, copper, carbon cement or graphite, and several routes have been devised to apply the electrodes to the target surface, including electroplating [4], painting [46], sputtering [46] and printing [23, 29]. Copper electroplating [42] has been reported to have high repeatability and durability [4] but the method requires uniform removal of the surface resin. Indeed, weaker adhesion forces often develop at the copper/resin interface thereby which leads to debonding and malfunctioning. Moreover, since the current flows only through the carbon fibers that are in contact with the electrode,

large zones of unpolished surface resin can lead to non-homogeneous current flow through the material. It is apparent that proper surface preparation is a crucial step in the quality of the output from the electrodes.

Surface preparation is usually accomplished by sanding [4], which involves manual removal of the resin layer through the use of several grades of sand paper. Previous studies have described the limitations of sanding [51]: it is a manual technique that is dependent on the operator and which leads to non-repeatable results. In addition, it is also time consuming and may induce damage on the exposed surface of the laminate. Therefore, alternative techniques are needed to overcome these limitations. From this standpoint, pulsed laser irradiation has recently been shown to be a very effective surface modification technique for a variety of materials. For instance, it can be used to improve adhesion between metals and epoxy resin [39, 40], but also for precision material cutting and/or drilling [36] on a variety of materials including composites [59, 54, 43]. Moreover, it has been recently employed to enhance the tribological behavior of steel and diamond coatings [41, 58].

With carefully selected processing parameters (*e.g.*, laser wavelength, average power delivered by the laser beam, pulse duration and frequency, laser scanning speed), laser irradiation is able to remove material through photochemical (photolytic) or photothermal (pyrolytic) processes or a combination of both [7]. In photochemical ablation, the bond excitation above a certain limit induce material dissociation. This process is characteristic of lasers with short wavelengths, such as UV lasers [19]. At longer wavelengths, the applied energy is not high enough to induce the photolytic process and hence is absorbed into the material as vibrational energy or heat. When the temperature reaches the vaporization temperature of the material, the material evaporates or sublimates [19]. Extensive surface modifications occur only when the applied energy reaches a certain threshold, which depends on the target material as well as the selected laser processing parameters. In the case of CFRP, the properties of the primary constituents vary dramatically. The laser's parameters thus need to be carefully tuned to selectively remove the polymer matrix with little or no fiber damage [50].

Here we propose the use of laser irradiation, in place of sanding, in the preparation of

high-quality electrodes for EIT. In particular, we identify suitable laser processing parameters that allow the selective removal of surface resin with negligible fiber damage, and we compare the quality of the electrodes prepared using laser irradiation and sanding in terms of electrode/substrate contact resistance. The remainder of the paper is organized as follows. A short review of EIT and electrical monitoring of CFRP is provided in Section 2. In Section 3, the experimental investigations, including the protocols to fabricate and test the different types of electrodes, are described. The results presented in Section 4 include both a detailed morphological analysis of the surface (to assess the removal of the resin from the prepared surface) and an evaluation of the electrical resistance of the tested electrodes.

2. Impedance-based CFRP composite characterization

Three methods have been proposed for CFRP composite characterization, *i.e.* electrical resistance change method (ERCM) [34, 5, 6], electrical impedance spectroscopy (EIS) [32, 17, 57] and electrical impedance tomography (EIT) [28, 15, 56].

The electrical resistance change in carbon fiber reinforced polymers (CFRP) is useful in monitoring damage initiation. Many researchers have utilized the electrical resistance change method to detect damage in CFRP composites [34, 5, 6]. ERCM applies a DC or AC current with constant amplitude at a particular frequency and measures the surface potential (Fig. 1a) to calculate the resistance of the material using four electrodes [57].

Electrical impedance spectroscopy (EIS) [32, 17, 57] measures electrical impedance of the CFRP part from the voltage-current data collected at the object boundary (Fig. 1b) at different signal frequencies (f). A constant amplitude sinusoidal electrical current is injected at different frequencies to identify the change in frequency of the impedance (Z) of the sample. EIS has been used in noninvasive material characterization of different composite materials [31, 27, 33, 26] including fibre-reinforced polymers [33]. EIS has also been found to be useful in monitoring the cure of plastics [26] during their manufacturing process. Recently, CFRP composites have been characterized by EIS and the preliminary results have been reported [53, 44, 20, 22].

Electrical Impedance Tomography (EIT) is a computed tomographic technique that provides 2D or 3D reconstructions [49, 16] of the spatial distribution of the electrical properties of a domain (Ω). It relies on voltage-current data measured at the domain boundary ($\partial\Omega$), which is mapped by an array of electrodes (Fig. 2). EIT is a low-cost, non-invasive and non-ionizing imaging technique. It has been used in medical diagnosis, industrial process tomography, civil engineering, geotechnology, material engineering, and biotechnology.

In ERCM, EIS and EIT, voltage-current data are required to obtain the resistance or impedance parameters of the composite structure and hence an array of sensors or electrodes must be placed on the material's surface to create an interface between the material and the instrumentation system. Because CFRP materials are composed of conducting carbon fibers embedded in an insulating resin, the placement of electrodes on a CFRP surface is not only a difficult task but it also plays a significant role in the accuracy of the measurements, the quality of the data and all final results. We propose herein a novel electrode fabrication method that facilitates the placement and connection of the electrodes on CFRP composite materials in ERCM, EIS, EIT or any other resistance (or impedance) analyzing techniques.

3. Materials and methods

3.1. Fabrication of composite laminates

The laminates used in this study were obtained from carbon fiber prepregs made of a toughened epoxy resin and supplied by Hexcel Composites (HexPly M21/ 35%/ 268/ T700GC). The resin and fiber densities were 1.28 and 1.80 g/cm^3, respectively, and the nominal fiber volume fraction was 56.9 %. Unidirectional ($[0]_8$) and cross-ply laminates ($[0°/90°]_{2s}$) were fabricated by compression molding of prepreg sheets. The following curing cycle was used: (1) full vacuum at 1 bar was applied to the whole stack to avoid air entrapment and the formation of voids; (2) 7 bar gauge pressure was then applied through a hydraulic hot press machine (Laboratory Press 15T, PEI France) at 180°C for 120 minutes; (3) the laminate was cooled down at 2°C/min intervals. The obtained composite laminates were used as substrates for the subsequent parametric study of the effects of laser processing parameters and for electrical contact resistance measurements.

3.2. Surface pretreatment

Laser ablation was carried out using a ytterbium (Yb) fiber laser (1064 nm wavelength) using a PLS6MW multi-wavelength laser platform (Universal Laser Systems, USA). The main processing parameters of the system were: laser maximum average power (P_{ave}): 30 W; pulse frequency (f): 30 kHz; pulse duration (τ_p): $\geq$10 ns; minimum line spacing (p): 30 μm; maximum scanning speed (v): 500 mm/s; focused beam diameter (d_s): 25 μm. The pulse fluence that was transmitted to the target surface can be obtained as a function of the main processing parameters:

$$F_p = I_p \cdot \tau_p = \frac{P_{ave}}{f A_s}, \tag{1}$$

where I_p is the pulse irradiance and A_s is the effective focal spot area. In the subsequent experiments, selected values of the average power and laser scanning speed were specified as percentages of the maximum values allowed by the system. In particular, to finely tune the laser irradiation, the power was varied within $15\% - 25\%$ of the maximum average power by steps of 2.5% while the laser speed was varied between $10\% - 20\%$ of the maximum speed by steps of 1%. This range was narrowed based on the results of preliminary experiments carried out in wider power and speed ranges. For this parametric study, ($5\ mm \times 5\ mm$) square arrays were processed on a cross-ply substrate by varying the laser's power and speed (Fig. 3), giving rise to fifty-five combinations of (P_{ave}, V). These preliminary tests were used to select the optimal combination of laser processing parameters in the fiber direction to achieve uniform surface resin removal and limited fiber damage. Subsequently, these laser parameters were replicated onto $5\ mm \times 20\ mm$ rectangular areas allocated for electrode fabrication.

The sanding procedure outlined in [4] was followed. In particular, $5\ mm \times 20\ mm$ areas were delimited using surface masking with vinyl tape[1] and then the areas were treated with two grades of sand paper (SiC-paper grit 320 and 1000, Struers). The sanding was carried out parallel to the fibers direction. A few drops of concentrated sulfuric acid (97%) were

[1]Notice that contrary to laser ablation, precise control of the treated area was not possible, for this reason masking was carried out beforehand.

then applied to complete the process, followed by extensive cleaning with distilled water and acetone.

3.3. Survey of surface morphology and chemistry

The quality of the processed surfaces was analyzed using optical microscopy (OM) on a stereomicroscope (Leica S6D, Germany). In addition, a high-resolution Scanning Electron Microscope (SEM) was used to analyze the surfaces (FEI Quanta 200). The cross-sections of treated samples were studied with an optical microscope (Leica DM2500 M, Germany). To prepare the cross-sections, samples were embedded in epoxy resin (EpoFix, Struers) and, after curing, they were cut and polished to enhance imaging.

Since optical and scanning microscopy deliver only qualitative assessments of the treated surfaces, Raman spectroscopy was also used to complement the surface analysis with information concerning the chemical composition. A Raman spectrometer (LabRAM Aramis, Horiba Scientific Ltd) was used to probe the samples in the range of $1000 - 1700$ cm^{-1}. A diode-pumped solid-state (DPSS) laser with a wavelength of 785 nm was used as the excitation source (low photon energy was necessary to avoid excessive fluorescence of the resin). A 600 groves/mm dispersive grating combined with thermoelectrically cooled, silicon charge-coupled device detector achieved a spectral resolution of approximately $1cm^{-1}$. The laser power on the sample surface was fixed at 0.07 mW to avoid the heating effects on the sample. A 50X long work distance lens with a numerical aperture (N.A.) of 0.5 was used to focus the laser and collect scattered light. The size of the laser spot was around $1\mu m$. The exposure time on single spot was 100s. A 3-axis (XYZ) motorized stage with a minimum step of $0.1\mu m$ was used to mount samples which allowed sample movement precisely along the line in the line scan measurements. The Raman spectra for pure epoxy, pure carbon fiber and the composite (resin+fiber) are shown in Fig. 4(a). As shown in Fig. 4(a), pure epoxy is characterized by two peaks at around 1147 cm^{-1} and 1585 cm^{-1}. Similarly, carbon fiber is characterized by two broad bands at 1330 cm^{-1} and 1610 cm^{-1}. The presence of carbon and epoxy together is indicated by three distinct peaks, which combine the peaks of pure carbon fiber and epoxy (1147 cm^{-1}, 1330 cm^{-1} and 1610 cm^{-1}). Depending on the

location and number of peaks, a spot is classified into three categories: pure carbon fiber, pure epoxy or a mix of the two. The Raman scanning was carried out perpendicular to the fibers over a line with a length of 400 μm. The samples were mounted on a 3D automatic stage for the line-scan Raman measurements. The stage was displaced automatically along the selected line on the sample surface while the spectrometer recorded the Raman spectrum for each collection point. Each collection point had a spot size of 2 μm in diameter and the sample stage moved 2 μm, thereby resulting in 200 acquisition points along the selected scanning line. Raman scanning provides quantitative results about the surface quality in terms of fiber exposure, as shown in Fig. 4(b).

3.4. Electrode fabrication

To analyze the contact resistance, we prepared six unidirectional composite laminates (270 mm $\times$ 20 mm $\times$ 2 mm). Three samples were surface treated using laser irradiation while the remaining three samples were manually sanded. In both cases, the targeted areas for electrode placement was 5 mm $\times$ 20 mm while the spacing between the areas' center points was 25 mm as shown in Fig. 5. Sets of electrodes were fabricated by three different techniques: (*i*) copper electroplating (*ii*) copper electroplating with a seed layer and (*iii*) silver paste.

3.4.1. Copper electroplating

Copper electroplating was performed on the treated surfaces by mainly following the procedures outlined in [4] with the main difference the surface preparation method. The substrate surfaces were delineated using vinyl tape such that only the areas allocated for electrode placement (5 mm $\times$ 20 mm) were exposed. The taped samples were placed in a copper sulfate (Cu_2SO_4) solution along with a copper plate. A low current density ($0.66A/dm^2$) was then supplied for 120 minutes to obtain an initial uniform thin copper layer over the targeted areas. After that, lead wires were bonded to the copper layer with a conductive epoxy adhesive (ITW Chemtronics, USA). After the adhesive was cured, the sample was again placed in the copper sulfate solution and a higher current density ($6A/dm^2$) was applied for 90 minutes to fully cover the wires. In this way it was possible to avoid the

occurrence of thermal stresses induced by soldering. As a final step, the tape was removed from the sample and a non-conductive epoxy adhesive was applied to cover the electrodes to protect them from environmental conditions and potential damage induced during sample handling.

3.4.2. Copper electroplating with a seed layer

To improve the growth of the electroplated copper, Todoroki *et al.* [4] used silver paste as a seed layer. Here, we used copper as a seed layer through copper deposition of two samples. The samples were covered with a vinyl tape to expose only the areas targeted for the deposition. Afterward, a 1-μm layer of copper was deposited for 50 minutes using an e-beam evaporator (Denton Vacuum Inc, USA). The tape was then removed, and new tape was applied for the copper electroplating process, as described in Subsection 3.4.1, during which low current density and high current density baths were used.

3.4.3. Silver paste

The procedure used to make electrodes using silver paste (Electron Microscopy Sciences, USA) was as follows. Surface-treated substrates were masked with vinyl tape and then the silver paste was applied to the unmasked locations for electrode fabrication. Wires were then bonded to the silver paste by means of a conductive epoxy adhesive. After the adhesive was cured the mask was removed and the sample was cleaned with acetone. Finally, following the same procedure as the earlier samples, the electrodes were covered with a protective layer of standard epoxy resin.

3.5. Measurements of electrical contact resistance

During the electrical measurements, an alternating current of 450 Hz and 30 mA was supplied while the impedance was measured using a LCR meter (Agilent-E4980A Precision LCR meter, measurement precision: $1e^{-7}\Omega$). Since the phase angle was negligible, the measured impedance was considered to be equal to the electrical resistance. The electrical resistance measurements were carried out using two-probe and three-probe methods to evaluate the electrical contact resistance of the electrodes.

In each laminate, we use set of 3 electrodes to measure the contact impedance of the middle electrodes as shown in Fig. 5. For each set of 3 electrodes (for eg: I_1, A, B):

1. current is injected in the outer electrodes (namely: I_1 and B) followed by measuring the electric potential between the first and second electrodes (namely: I_1 and A). This is a three-probe measurement.

2. current is injected and electric potential is measured between the first and the second electrodes (namely: I_1 and A). This is a two-probe measurement.

The difference between the two electric potentials gives the contact impedance of the middle electrode (A). The process is carried out through subsequent three-pairs of electrodes to estimate the contact impedance of the electrodes (A, B, C, D and E). The variation in the measured contact impedance is plotted to evaluate the repeatability.

4. Results and discussion

4.1. Assessment of modifications in the surface morphology

Optical and SEM images of sanded surfaces, which are shown in Fig. 6(a) and (b), respectively, demonstrate the unevenness of the obtained surface. Indeed, epoxy residue can be observed around the edges of the treated area. This is because the quality of the surface finish cannot be guaranteed by a manual process. This is one of the main drawbacks of this method as it suffers from operator-to-operator variability. This is highlighted by the SEM image in Fig. 6(c), which shows a significant amount of epoxy resin that was not removed from the surface as well surface fibers that were damaged during the process (see insert). Both drawbacks were systematically observed in all sanded surfaces. Figure 7(a) shows an actual cross-sectional view of a sanded surface as well as a schematic that emphasizes the main attributes of the surface, *i.e.*, the non-uniform removal of the surface resin and the induced fiber damage.

Fig. 8 shows the various combinations of laser processing parameters along with optical microscopy observations of selected surfaces that were treated with laser irradiation. We

grouped the treated surfaces into three categories: R, surfaces with poor surface resin removal; D, surfaces with fiber damage; I, surfaces with efficient resin removal. It is apparent that higher laser power/frequency results in high incident energy into the material and that lower laser speed results in higher duration of the local interaction with the material. It follows an increased heat absorption which leads to a high local temperature and, fiber vaporization. Indeed, it should be noted that when the surface of CFRP is subjected to laser irradiation, the energy delivered to the surface is absorbed, excites the bonds and generates heat. Since the carbon fibers are thermally more conductive than the matrix, the absorbed heat conducts along the fibers, increasing the temperature locally along the direction of the fibers. Once the temperature reaches the vaporization temperature of the matrix, the matrix along the conduction path evaporates. This zone where the matrix loss occurs due to photothermal conduction is known as the heat-affected zone (HAZ) [52]. It has been shown that the size of the HAZ depends on the laser scanning speed, direction, power and frequency as these variables determine the energy absorbed into the material [52, 30]. Figure 8 also shows optical images taken from three selected regions that are representative of the three groups mentioned above. In addition, Fig. 9 shows the corresponding SEM images. Extensive fiber damage occurred in the samples that were exposed to either high laser power, slow laser speed or both. This is because at high power or at low speed, the amount of energy absorbed locally is high enough to induce fiber damage. Similarly, samples processed at high laser speeds or low laser power exhibit poor surface resin removal as the local energy density is not high enough for the surface removal to occur. The samples in the intermediate range exhibit resin removal with apparent minimal damage. Fig. 7(b) shows the actual cross-sectional view of the laser treated samples as well as a schematic highlighting that the process was able to remove the resin effectively. The cross-sectional views (Fig. 7 (a) and (b)) show that the surface obtained as a result of laser ablation is rougher than that obtained using sanding. High surface roughness is usually attributed to better interlocking and can result in better adhesion between two joining surfaces (the electrode and the laminate) [39, 40]. Thus, we believe that laser irradiation also increases the durability of the contact between the electrode and laminate.

4.2. Analysis of the surface chemistry using Raman spectroscopy

A typical response recorded during Raman line scanning of a sanded sample is provided in Fig. 10 (a). The intensity counts were distributed as follows: 25% for carbon fibers, 38.5% for pure epoxy and 36.5% for the combination of both. Analysis of these results demonstrates that with sanding, the percentage of fully exposed fibers is very low and that most of fibers are covered with a very thin layer of resin. Raman line scanning was also carried out on the laser-treated samples from the three categories. Here, we show the results obtained from the sample prepared at $V = 15\%$ and P_{ave}=22.5% (Fig. 10 (b)). It is notable that samples from the same category (I) exhibited similar results whereas results from category (R) exhibited a very low percentage of exposed fibers. The intensity counts were distributed as follows: 77.5% for fully exposed carbon fibers, 9% for pure epoxy and 13.5% for the combination of both. Therefore, a remarkable improvement in the percentage of fully exposed carbon fibers compared with sanded samples was achieved. There were still areas where the carbon fibers were not completely exposed, which is also captured in the SEM images of the surfaces, *i.e.* Fig. 9(d), but the percentage was very low in comparison to the number of fully exposed fibers. We believe that the obtained fiber exposure is sufficient for the purposes of the study. Hence the combination of the parameters in the intermediate range are selected as the optimal range. For subsequent electrode fabrication, the combination V=15% and P=22.5% was chosen.

4.3. Analysis of electrical contact resistance

Figures 11 and 12 show the electrical contact resistance values of the sanded samples and the laser-ablated samples for different electrode materials, respectively. The figure shows the calculated electrical contact resistance of the five inner electrodes (A-E, marked in the abscissa) based on the difference between the two-probe and three-probe measurements. It can be seen that the electrical contact resistance of the sanded surfaces (average 0.325 Ω) is about five times the electrical contact resistance of the laser-ablated surfaces (average 0.067 Ω). Also, the sanded samples exhibit large variations in the measured contact impedance

(around ± 0.06 Ω) thereby indicating low repeatability. In comparison, the laser-treated samples exhibit high repeatability with very low variation (around ± 0.01 Ω).

The sanded samples exhibited high variations in the contact impedance depending on the electrode material used (20.3% relative variation). These variations are, we believe, due to the inhomogeneity in the sanded samples. However, the laser-ablated samples exhibited little variation in terms of the electrode material (4.1% relative variation). These results suggest that the contact impedance mainly depends on the method of surface preparation and is independent of the electrode material. This is advantageous as silver paste is superior in terms of scalability, ease of processing and cost when compared to copper plating. Thus, silver paste can be used instead of copper electroplating to prepare the electrodes. Although we did not study the durability, we believe that the surface roughness obtained through laser ablation provides improved interlocking and hence greater durability irrespective of the electrode material used. This suggestion has to be experimentally validated.

5. Conclusion

This study focused on developing a new method for surface preparation of composite laminates for better electrode quality in EIT. We obtained proper laser parameters with minimal surface fiber damage. We also characterized the surfaces using microscopic imaging, SEM and Raman spectrum mapping. The results showed that the electrical contact resistance of the sanded samples (average 0.325 Ω) is about five times the electrical contact resistance of the laser-ablated surfaces (average 0.067 Ω). All the electrode materials had very low and almost the same electrical contact resistance measurements in the laser-ablated samples. The variation in electrical contact resistance measurements of the laser-ablated samples was very low when compared with that of the sanded samples. Future studies will focus on the durability of the electrodes obtained by this process.

References

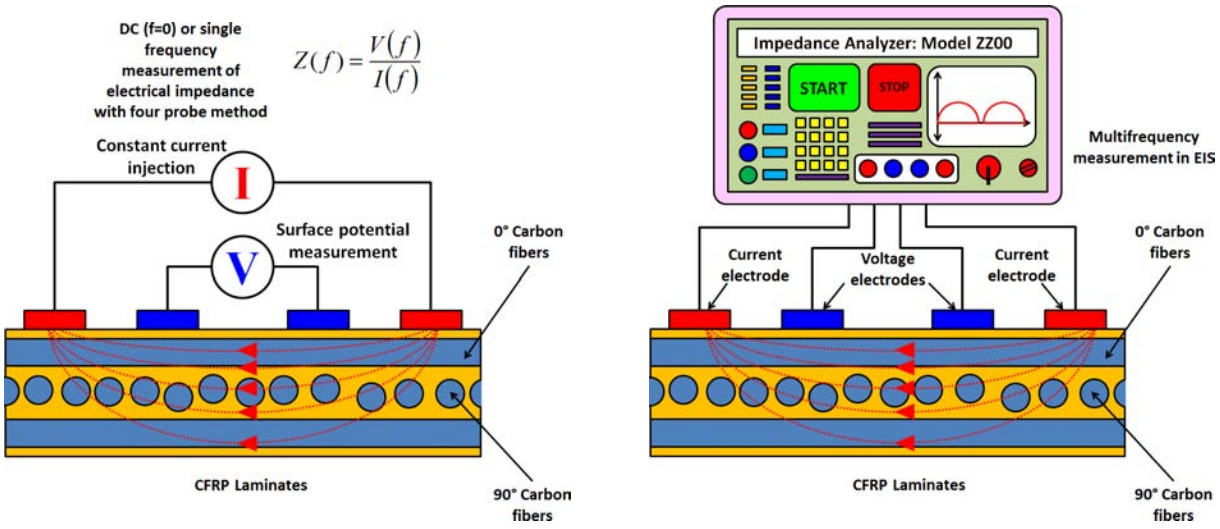

(a) **(b)**

Figure 1: (a) Schematic representation of the electrical resistance change method for CFRP composite characterization; (b) schematic diagram of the impedance measurement in electrical impedance spectroscopy (EIS).

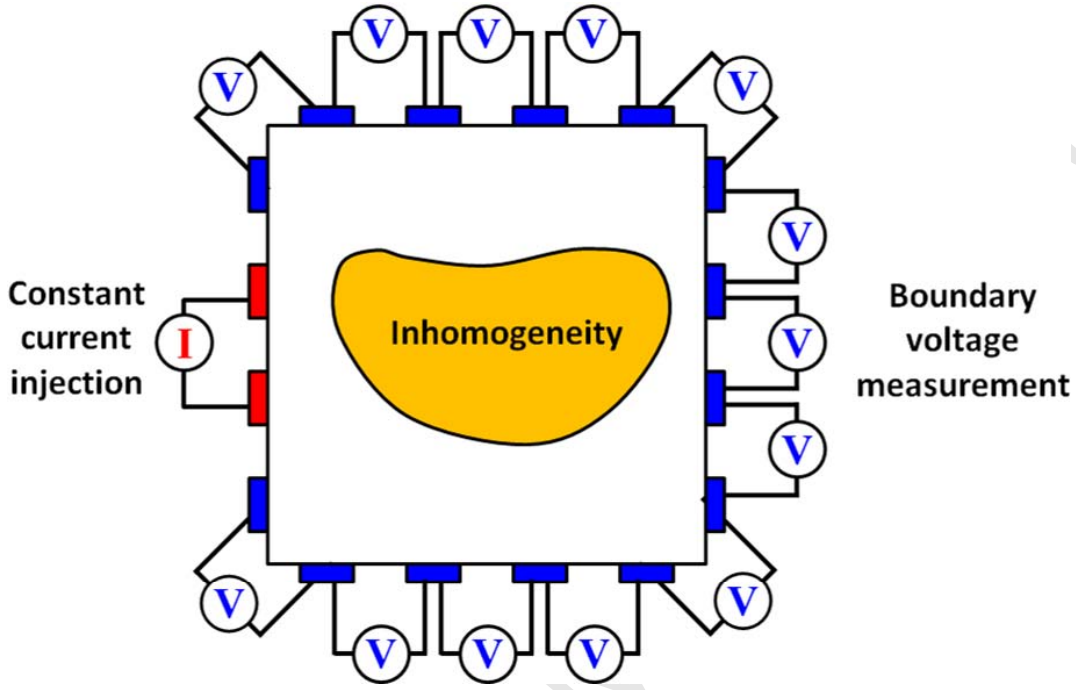

Figure 2: Schematic diagram of boundary data collection in electrical impedance tomography (EIT).

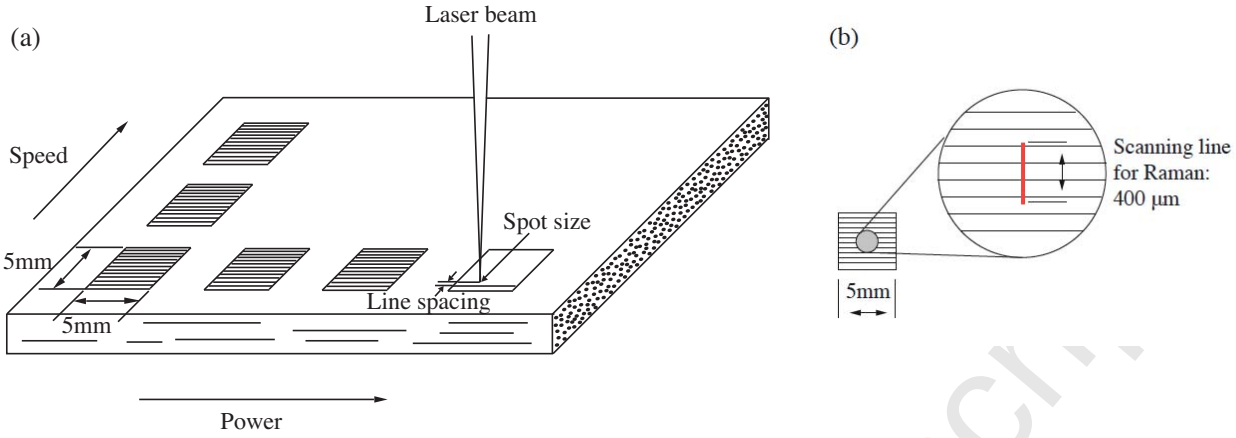

Figure 3: (a) Schematic depiction of the electrode array employed to probe the di erent laser processing con gurations; (b) location of the Raman survey line for each processed surface.

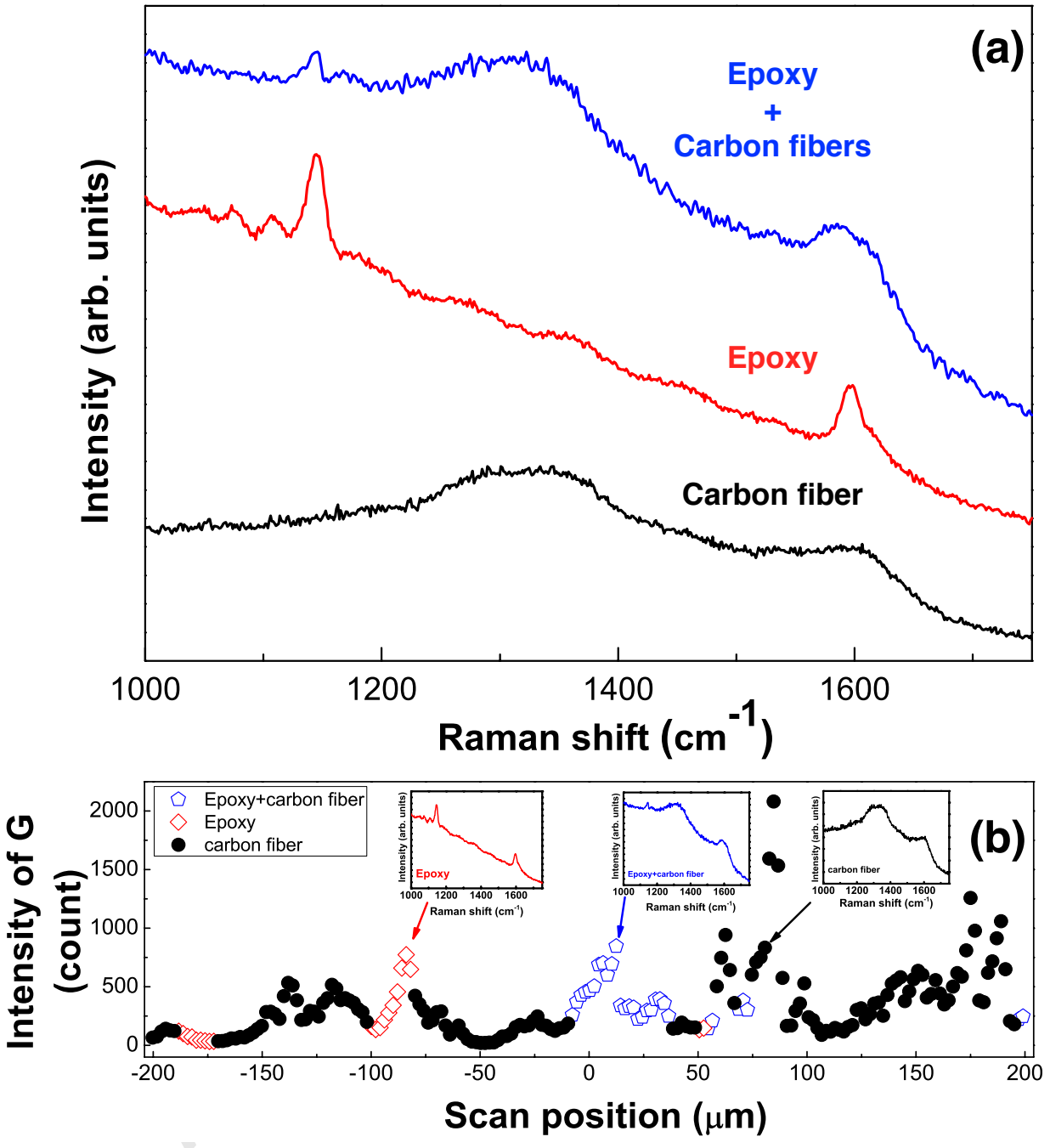

Figure 4: (a) Raman spectra of carbon ber, epoxy and epoxy+carbon bers; (b) Line scan and the corresponding Raman spectrum of each point.

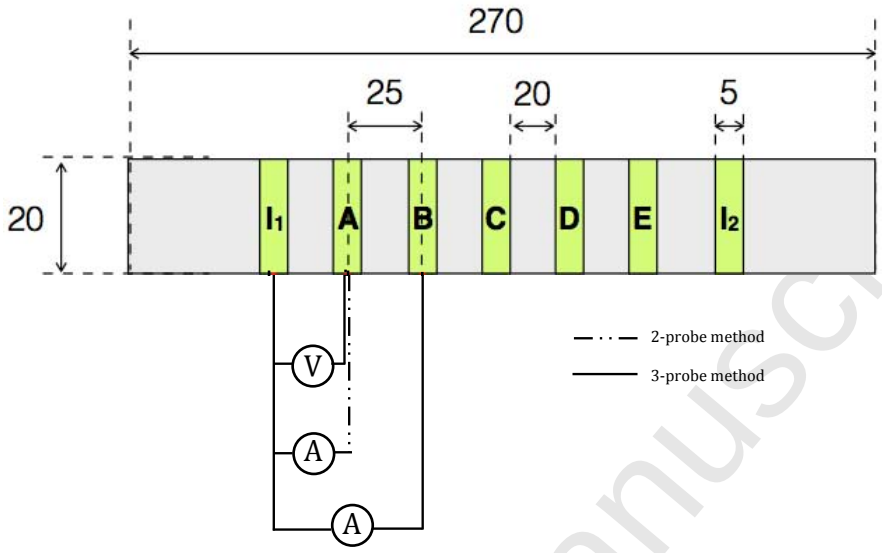

Figure 5: Con guration of the electrodes on an 8-ply unidirectional (UD) laminate with a schematic of the two-probe and the three-probe methods.

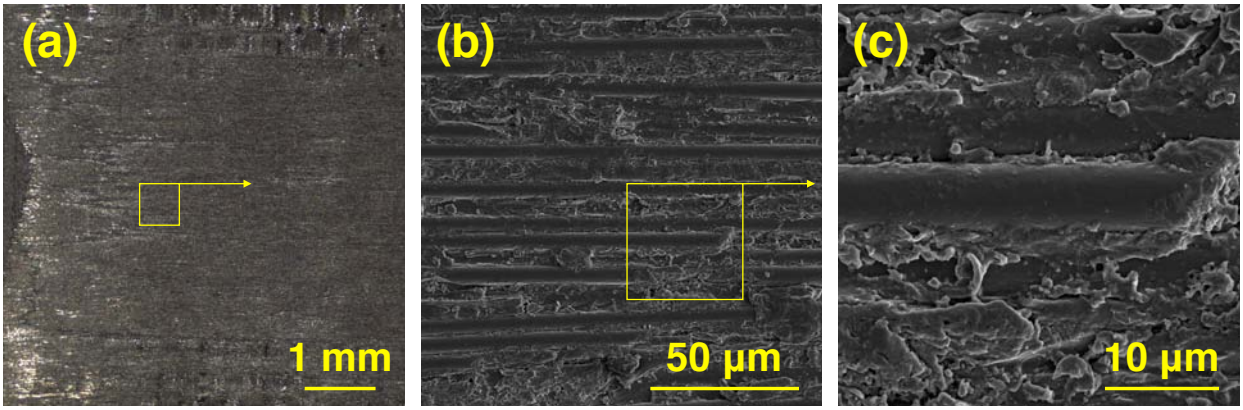

Figure 6: (a) Optical microscopy image (40X mag.) and (b) SEM image of a sanded surface; (c) is a magni cation of the inset in (b).

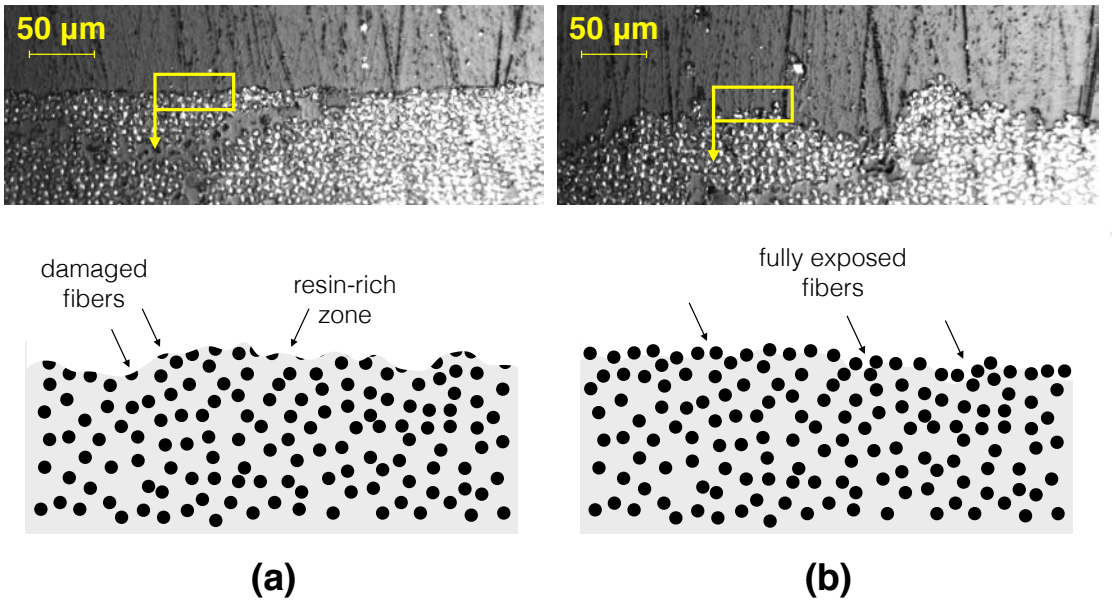

Figure 7: (Cross-section and corresponding schematic of processed surfaces by (a) sanding and (b) laser ablation.

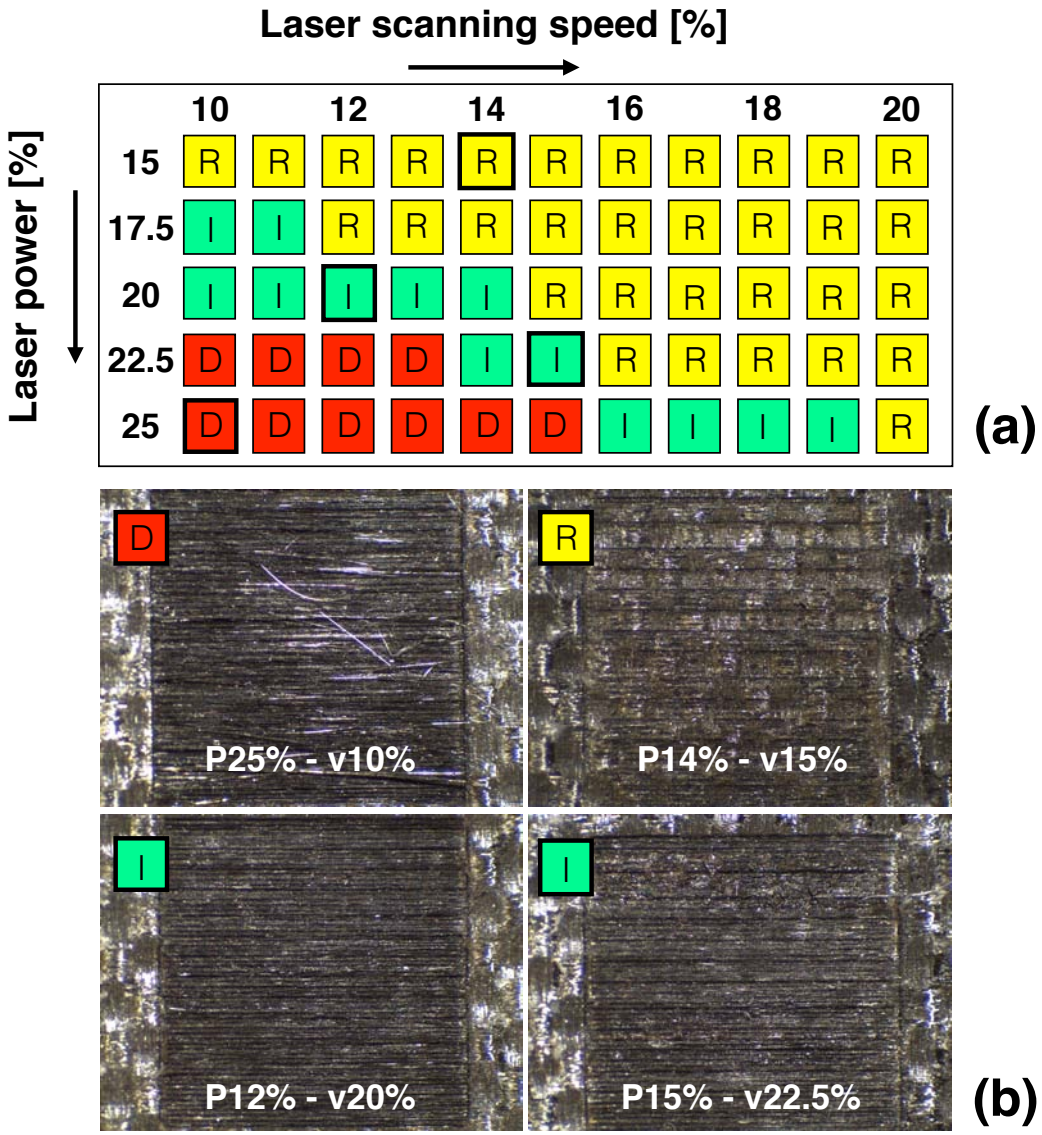

Figure 8: (a) Broad classi cation of the electrode surfaces based on optical pictures; (b) Optical images (10X mag.) of the samples from the three regions (D: surfaces with ber damage; R: surfaces with poor resin removal; I: surfaces with e cient resin removal).

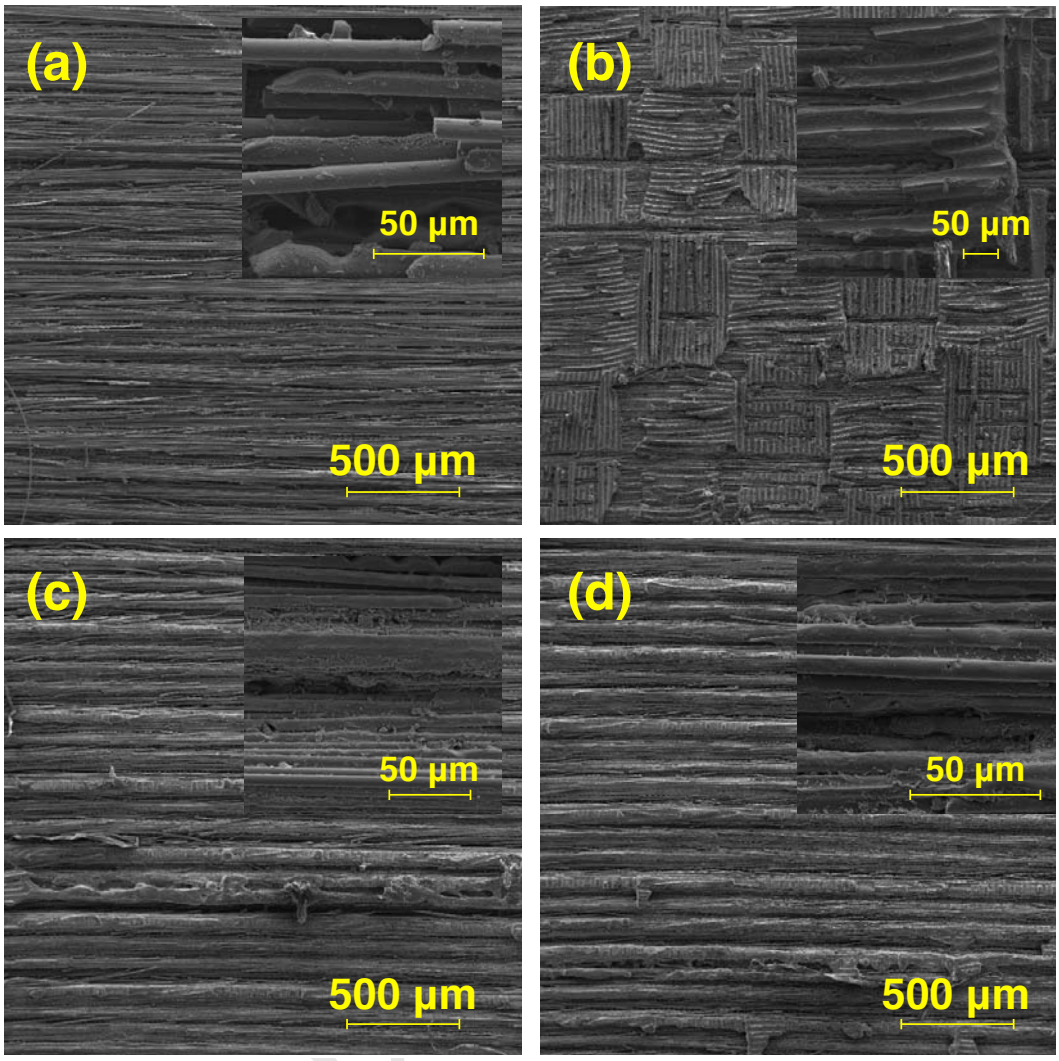

Figure 9: SEM images of the samples from three regions: (a) a surface with extensive ber damage; (b) a surface with minimal surface resin removal; (c) and (d) surfaces from the intermediate range (insets: magni ed images).

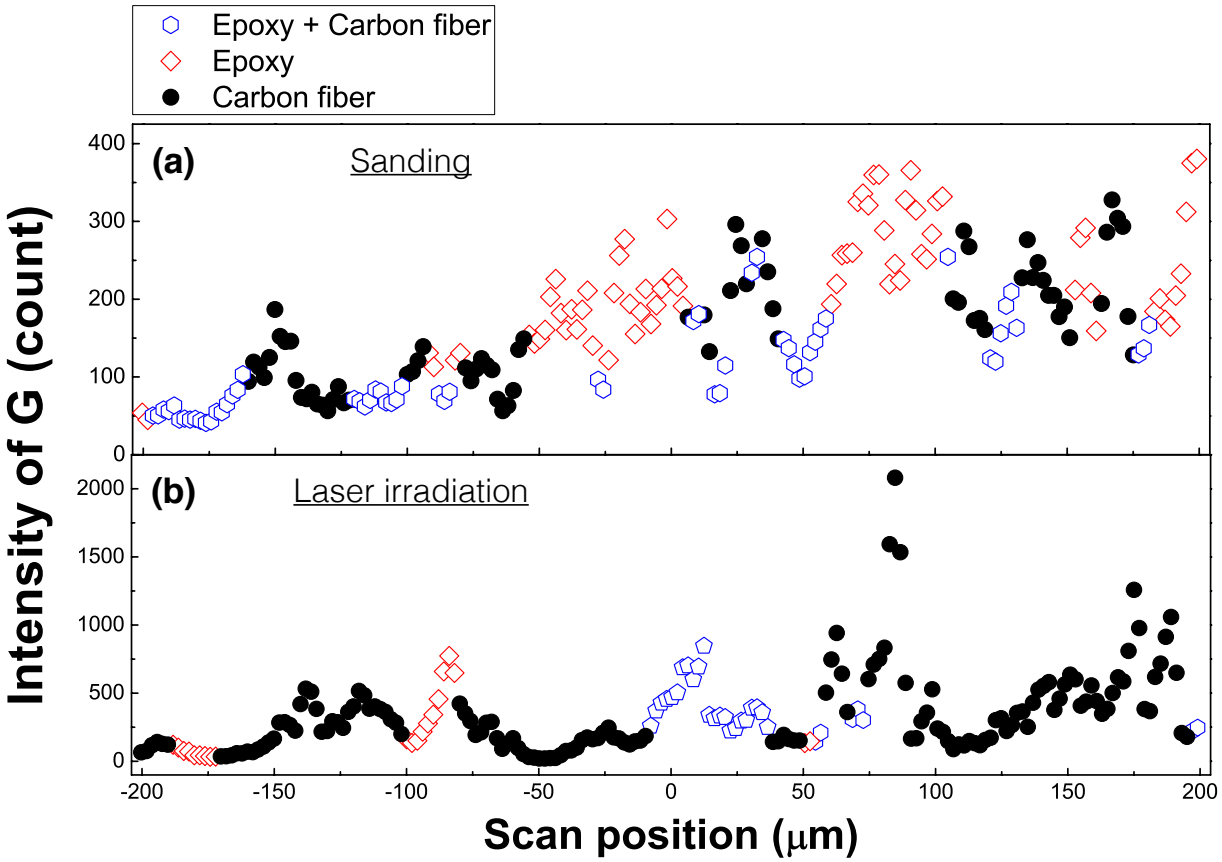

Figure 10: (a) Classi cation obtained by Raman imaging over a 400 μm line on a sanded sample; (b) Raman imaging over a 400 μm line on a laser-ablated surface at V = 15%; P = 22.5%.

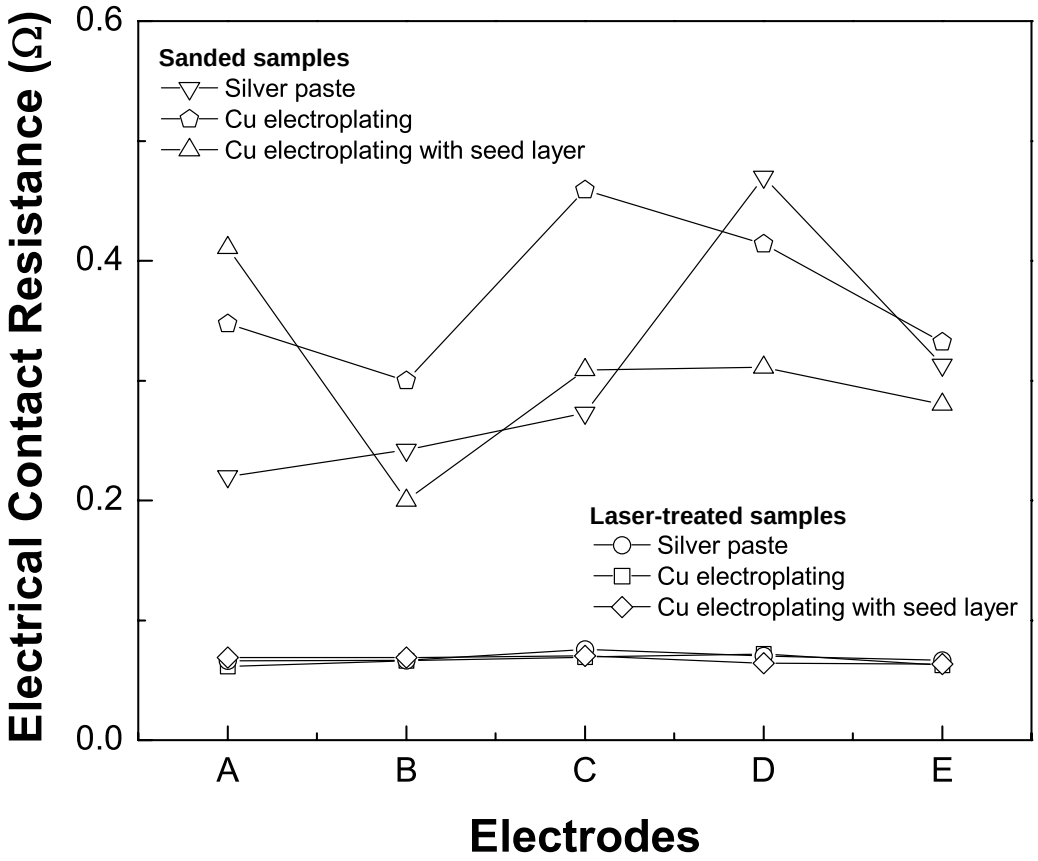

Figure 11: Electrical contact resistance of the ve inner electrodes in di erent electrode materials

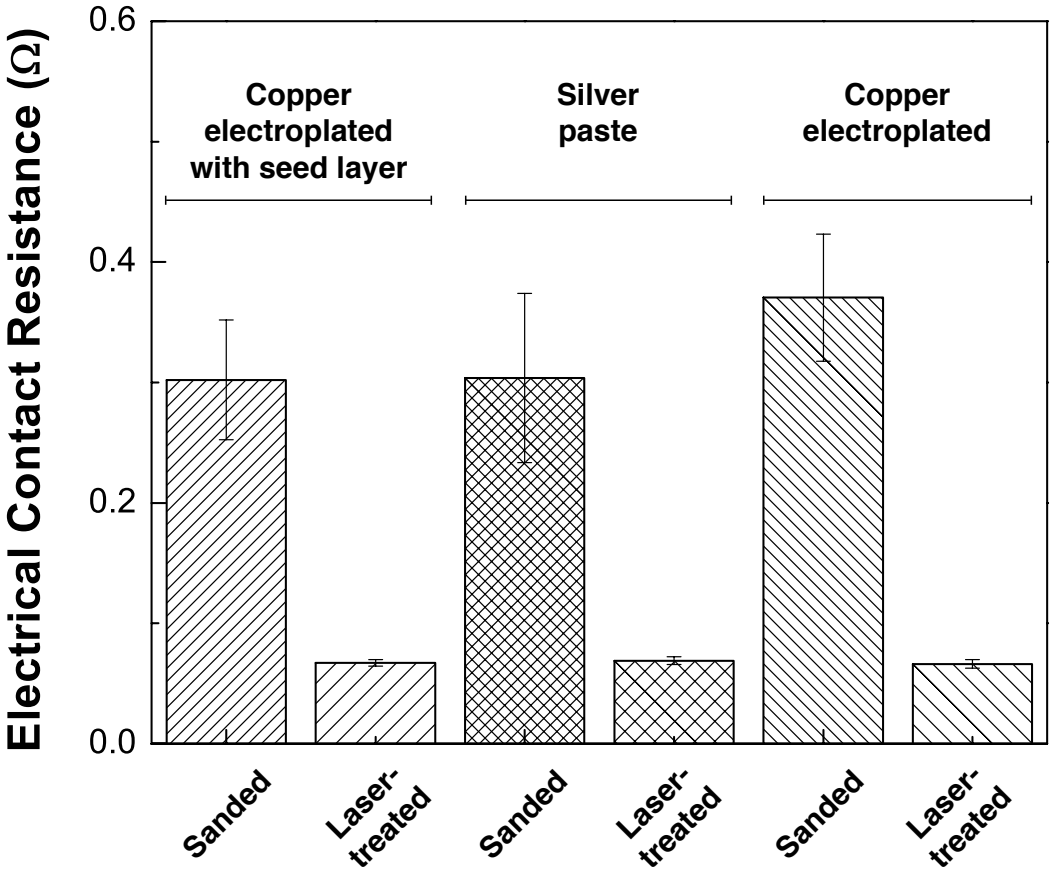

Figure 12: Electrical contact resistance of the laser-ablated and the sanded samples with di erent electrode materials

References

[1] A. Borsic, 2002. Regularisation methods for imaging from electrical measurements. Ph.D. thesis. Oxford Brookes University.

[2] A. R. Bunsell, 1983. Composite Structures 2. Springer. chapter The Monitoring of Damage in Carbon Fibre Composite Structures by Acoustic Emission. pp. 1{20.

[3] A. Todoroki, D. Haruyama, Y. Mizutani, Y. Suzuki, T. Yasuoka, 2014. Electrical resistance change of carbon/epoxy composite laminates under cyclic loading under damage initiation limit. Open Journal of Composite Materials 4, 22{31.

[4] A. Todoroki, K. Suzuki, Y. Mizutani, R. Matsuzaki, 2010. Durability Estimates of Copper Plated Electrodes for Self-sensing CFRP Composites. Journal of Solid Mechanics and Materials Engineering 4, 610{620.

[5] A. Todoroki, M. Ueda, Y. Hirano, 2007. Strain and damage monitoring of cfrp laminates by means of electrical resistance measurement. Journal of Solid Mechanics and Materials Engineering 1, 947{974.

[6] A. Todoroki, Y. Mizutani, Y. Suzuki, 2013. Fatigue damage detection of cfrp using the electrical resistance change method. International Journal of Aeronautical and Space Sciences 14, 350{355.

[7] B. Garrison, R. Srinivasan, 1985. Laser ablation of organic polymers: Microscopic models for photo-chemical and thermal processes. Journal of Applied Physics 57, 2909{2914.

[8] C. Boller, W. Staszewski, 2004. Health monitoring of Aerospace Structures. John Wiley and Sons, Ltd.

[9] C. Ciang, JR. Lee, HJ. Bang, 2008. Structural health monitoring for a wind turbine system: a review of damage detection methods. Measurement Science and Technology 19.

[10] C. Maierhofer, P. Myrach, M. Reischel, H. Steinfurth, M. Rllig, M. Kunert, 2014. Characterizing damage in cfrp structures using ash thermography in re ection and transmission con gurations. Composites Part B: Engineering 57, 35{46.

[11] C. Meola, G. Carlomagno, M. Valentino, C. Bonavolont, . Non destructive evaluation of impact damage in cfrp with infrared thermography and squid.

[12] C. Ng, M. Veidt, 2009. A lamb wave based technique for damage detection in composite laminates. Smart Materials and Structures 18, 1{12.

[13] C. Scarponi, G. Briotti, 2000. Ultrasonic technique for the evaluation of delamination on cfrp, gfrp, kfrp composite materials. Composites Part B: Engineering 31, 237{243.

[14] C. Toscano, A. Riccio, F. Camerlingo, C. Meola, 2012. Lockin thermography to monitor propagation of delamination in cfrp composites during compression tests, in: 11th International Conference on Quantitative InfraRed Thermography, Naples, Italy.

[15] D. S. Holder, 2004. Electrical impedance tomography: methods, history and applications.

[16] D. Sbarbaro, M. Vauhkonen, T. Johansen, 2015. State estimation and inverse problems in electrical impedance tomography: observability, convergence and regularization. Inverse Problems 31.

[17] E. Barsoukov, J. R. Macdonald, 2005. Impedance Spectroscopy: Theory, Experiment, and Applications. Wiley-Interscience.

[18] F. Aymerich, S. Meili, 2000. Ultrasonic evaluation of matrix damage in impacted composite laminates. Composites Part B: Engineering 31, 1{6.

[19] F. Fischer, S. Kreling, P. Jaschke, M. Frauenhofer, D. Kracht, K. Dilger, 2012. Laser surface pre-treatment of CFRP for adhesive bonding in consideration of the absorption behaviour. The Journal of Adhesion 88, 350{363.

[20] G. D. Davis, 2013. Evaluating adhesive bonds with carbon-composites using electrochemical impedance spectroscopy.

[21] G. Lubineau, H. Nouri, F. Roger, 2013. On micro-meso relations homogenizing electrical properties of

transversely cracked laminated composites. Composite Structures 105, 66{74.

[22] G. Slipher, R. Haynes, J. Riddick, 2014. Experimental Mechanics of Composite, Hybrid, and Multifunctional Materials. Springer. volume 6. chapter Impedance Spectroscopy for Structural Health Monitoring.

[23] H-S. Kim, S. Dhage, Do-E. Shim, H. Hahn, 2009. Intense pulsed light sintering of copper nanoink for printed electronics. Applied Physics A 97, 791{798.

[24] HN. Li, DS. Li, GB. Song, 2004. Recent applications of ber optic sensors to health monitoring in civil engineering. Engineering structures 26, 1647{1657.

[25] I. De Rosa, C. Santulli, F. Sarasini, 2009. Acoustic emission for monitoring the mechanical behaviour of natural bre composites: a literature review. Composites Part A 40, 1456{1469.

[26] I. Perrissin-Fabert, Y. Jayet, 1994. Simulated and experimental study of the electric impedance of a piezoelectric element in a viscoelastic medium. Ultrasonics 32, 107{112.

[27] J. Ayres, F. Lalande, Z. Chaudhry, C. Rogers, 1998. Qualitative impedance-based health monitoring of civil infrastructures. Smart Materials and Structures 7, 599{605.

[28] J. G. Webster, 1990. Electrical Impedance Tomography (Adam Hilger Series on Biomedical Engineering). CRC Press.

[29] J. Kang, H. Kim, J. Ryu, H. Hahn, S. Jang, J. Joung, 2010. Inkjet printed electronics using copper nanoparticle ink. Journal of Materials Science: Materials in Electronics 21, 1213{1220.

[30] J. Mathew, G. Goswami, N. Ramakrishnan, N. Naik, 1999. Parametric studies on pulsed Nd:YAG laser cutting of carbon ber reinforced plastic composites. Journal of Materials Processing Technology, 89-90, 198{203.

[31] J. Pohl, S. Herold, G. Mook, F. Michel, 2001. Damage detection in smart cfrp composites using impedance spectroscopy. Smart Materials and Structures 10, 834{842.

[32] J. R. Macdonald, 1992. Impedance spectroscopy. Annals of Biomedical Engineering 20, 289{305.

[33] K. Nixdorf, G. Busse, 1998. Electrical impedance spectroscopy for cure monitoring and damage detection in model adaptive components, in: Euromech 373 Colloquium on Modeling and Control of Adaptive Mechanical Structures, Magdeburg, Germany.

[34] K. Schulte, C. Baron, 1989. Load and failure analyses of CFRP laminates by means of electrical resistivity measurements. Composites Science and Technology 36, 63{76.

[35] K. Telschow, C. Miyasaka, 2004. Fatigue damage evaluation in cfrp woven fabric composites through dynamic modulus measurements, in: ASME PVP 2004 International Conference, California, USA.

[36] L. Romoli, F. Fischer, R. Kling, 2012. A study on UV laser drilling of PEEK reinforced with carbon bers. Optics and Lasers in Engineering 50, 449{457.

[37] L. Selvakumaran, G. Lubineau, 2014. Electrical behavior of laminated composites with intralaminar degradation: a comprehensive micro-meso homogenization procedure. Composite Structures 109, 178{

188.

[38] L. Selvakumaran, Q. Long, S. Prudhomme, G. Lubineau, 2015. On the detectability of transverse cracks in laminated composites using electrical potential change measurements. Composite Structures 121, 237{246.

[39] M. Alfano, G. Ambrogio, F. Crea, L. Filice, F. Furgiuele, 2011. In uence of laser surface modi cation on bonding strength of Al/Mg adhesive joints. Journal of Adhesion Science and Technology 25, 1261{1276.

[40] M. Alfano, S. Pini, G. Chiodo, M. Barberio, A. Pirondi, F. Furgiuele, R. Groppetti, 2014. Surface patterning of metal substrates through low power laser ablation for enhanced adhesive bonding. The Journal of Adhesion 90, 384{400.

[41] M. Bieda, C. Schmdicke, T. Roch, A. Lasagni, 2015. Ultra-low friction on 100Cr6-steel surfaces after direct laser interference patterning. Advanced Engineering Materials 17, 102{108.

[42] M. Gigliotti, M.C. Lafarie-Frenot, Y. Lin, A. Pugliese, 2015. Electro-Mechanical Fatigue of CFRP Laminates for Aircraft Applications. Composite Structures 127, 436{449.

[43] M. Lima, J. Sakamoto, J. Simoes, R. Riva, 2013. Laser processing of carbon ber reinforced polymer composite for optical ber guidelines. Physics Procedia 41, 572{580.

[44] M. Mounkaila, T. Camps, S. Sassi, Ph. Marguers, Ph. Olivier, J.Y.Fourniols, C.Escriba, 2014. Cure monitoring of composite carbon/epoxy through electrical impedance analysis, in: Second European Conference of the Prognostics and Health Management Society 2014, Nantes, France.

[45] M. Perez, L. Gil, S. Oller, 2011. Non-destructive testing evaluation of low velocity impact damage in carbon ber reinforced laminated composites. Ultragarsas 66.

[46] N. Angelidis, C. Wei, P. Irving, 2004. The electrical resistance response of continuous carbon ber composite laminates to mechanical strain. Composites Part A: Applied Science and Manufacturing 35, 1135{1147.

[47] N. Polydorides, 2002. Image reconstruction algorithms in soft- eld tomography. Ph.D. thesis. University of Manchester Institute of Science and Tehnology.

[48] P. Boinard, R. Pethrick, W. Banks, R. Crane, 2000. Non destructive evaluation of adhesively bonded composite structures using high frequency dielectric spectroscopy. Journal of Materials Science 35, 1331{1337.

[49] P. Metherall, D. Barber, R. Smallwood, B. Brown, 1996. Three-dimensional electrical impedance tomography. Nature 380, 509{512.

[50] Q. Benard, M. Fois, M. Grisel, P. Laurens, 2006. Surface treatment of carbon/epoxy and glass/epoxy composites with an excimer laser beam. International Journal of Adhesion and Adhesives 26, 543{549.

[51] Q. Biao, 2009. Sanding, grit blasting and plasma etching: e ect on surface composition and surface energy of graphite/epoxy composites. Master's thesis. University of Cincinnati.

[52] R. Negarestani, M. Sundar, M. Sheikh, P. Mativenga, L. Li, Z. Li, P. Chu, C. Khin, H. Zheng, G. Lim, 2010. Numerical simulation of laser machining of carbon- bre-reinforced composites. Proceedings of the Institution of Mechanical Engineers, Part B: Journal of Engineering Manufacture 224, 1017{1027.

[53] R. Schueler, S. Joshia, K. Schulte, 2001. Damage detection in cfrp by electrical conductivity mapping. Composites Science and Technology 61, 921{930.

[54] R. Srinivasan, B. Braren, 1989. Ultraviolet laser ablation of organic polymers. Chemical Reviews 89, 1303{1316.

[55] S. Ramanan, A. Bulavinov, S. Pudovikov, C. Boller, 2010. Quantitative non-destructive evaluation of cfrp components by sampling phased array, in: 2nd International Symposium on NDT in Aerospace, Germany.

[56] T. K. Bera, 2012. Studies on Multifrequency Multifunction Electrical Impedance Tomography (MfMf - EIT) To Improve BioImpedance Imaging. Ph.D. thesis. Indian Institute of Science.

[57] T. K. Bera, 2014. Bioelectrical impedance methods for noninvasive health monitoring: A review. Journal of Medical Engineering 2014.

[58] T. Roch, V. Weihnacht, H. Scheibe, A. Roch, A. Lasagni, 2013. Direct Laser Interference Patterning of tetrahedral amorphous carbon lms for tribological applications. Diamond and Related Materials 33, 20{26.

[59] V. Tagliaferri, A. Di ilio, I. Visconti, 1985. Laser cutting of ber-reinforced polyesters. Composites 16, 317{325.

[60] Z. Su, L. Ye, Y. Lu, 2006. Guided lamb waves for identi cation of damage in composite structures: a review. Journal of sound and vibration 295, 753{780.

Sanded electrodes on CFRP

Laser ablated electrodes on CFRP

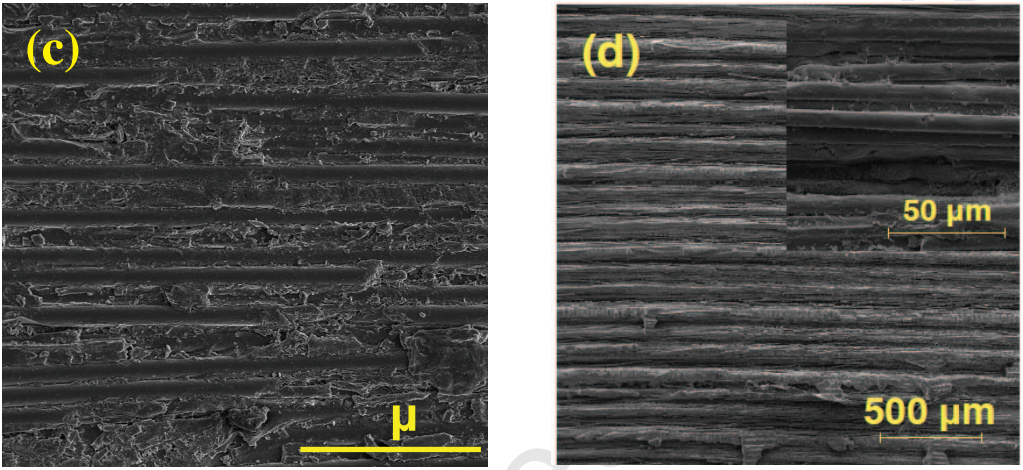

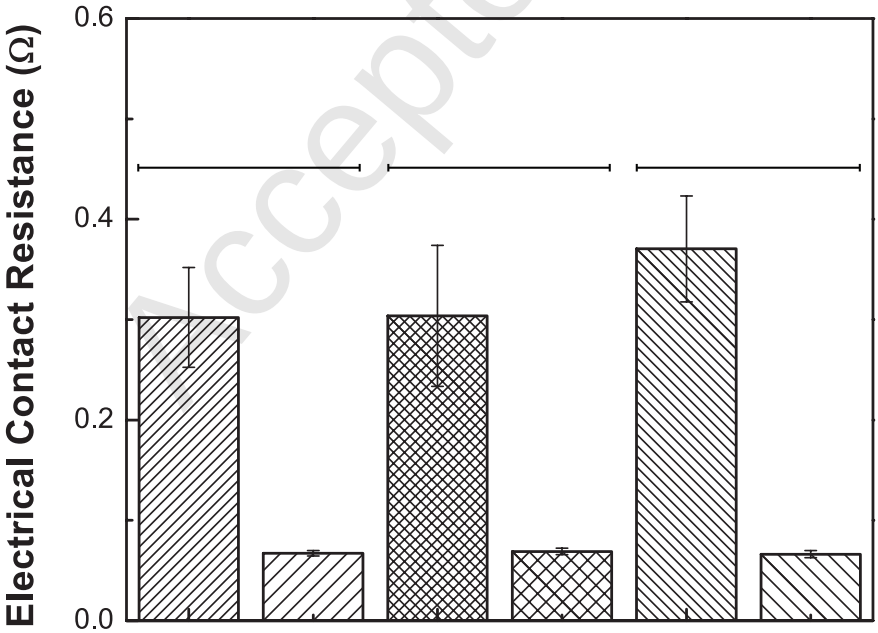

Highlights

- Laser ablation is proposed as an alternative surface preparation technique to sand polishing to prepare electrodes for electrical measurements in laminated composites
- Laser ablation provides better surface fiber exposure than sand polishing
- The optimal parameters for the laser ablation process is identified by qualitative assessment using Raman spectroscopy
- Electrodes produced over laser ablated surfaces show lower and uniform contact impedance in comparison to electrodes produced over sand polished surfaces
- Contact impedance is less dependent of the electrode conductive material when laser ablation is used for surface preparation